Nuclear Science and Techniques (2024) 35:90
https://doi.org/10.1007/s41365-024-01449-7

Cr-induced fusion reactions to synthesize superheavy elements

S. Madhu[1,2,3] · H. C. Manjunatha[4] · N. Sowmya[4] · B. M. Rajesh[1,2] · L. Seenappa[5] · R. S. Susheela[6]

Received: 10 October 2023 / Revised: 17 December 2023 / Accepted: 24 December 2023 / Published online: 3 June 2024

Abstract
We investigated $^{50,52-54}$Cr-induced fusion reactions for the synthesis of the superheavy element in the $104 \leq Z \leq 122$ range. The cross sections produced in this investigation using ^{54}Cr projectiles were compared with those obtained in prior experiments. The estimated cross sections from this analysis are consistent with the findings of prior studies. From the current study, the predicted cross section was found to be 42fb at 236 MeV for ^{53}Cr+^{243}Am, 23.2 fb at 236 MeV for ^{54}Cr+^{247}Cm, 95.6 fb at 240 MeV for ^{53}Cr+^{248}Bk, and 1.33 fb at 242 MeV for ^{53}Cr+^{250}Cf. Consequently, these projected cross sections with excitation energy and beam energy will be useful in future Cr-induced fusion reaction investigations.

Keywords Fusion cross sections · Compound nucleus formation probability · Survival probability · Evaporation residue cross sections

1 Introduction

The synthesis of superheavy elements has attracted considerable attention in the field of Nuclear Physics. Earlier it has been shown that superheavy elements can be produced in explosive stellar events, for example, the element with the proton number 110 was expected to be found in cosmic rays [1]. Since 1970, several attempts have been made to synthesize superheavy elements with the atomic number $Z \geq 110$ [2]. Using cold fusion reactions, elements with atomic numbers $Z = 107 - 113$ were synthesized using ^{208}Pb and ^{209}Bi as targets [3]. Element $Z = 112$ was synthesized by the bombardment of ^{208}Pb with ^{70}Zn [4]. The superheavy element tennessine $^{294}_{117}$Ts was synthesized via a ^{48}Ca-induced reaction with ^{249}Bk at the Dubna Gas-Filled Recoil Separator (DGFRS) in Dubna, Russia [5]. Further experiments were conducted to synthesize new superheavy elements from $Z = 113$ to 118 using the hot fusion technique [6, 7].

Many microscopic and macroscopic theoretical attempts were observed on the prediction of production cross sections. For instance, previous researchers studied the production cross section using the dynamic cluster decay model (DCM) for the superheavy element $Z = 116$ [8]. Using the dinuclear system (DNS) model [9], superheavy elements with $Z = 119$ and $Z = 120$ were investigated using Ca as a projectile with different target nuclei. Even though the systems ^{44}Ca+^{252}Es and ^{40}Ca+^{257}Fm yield larger production cross sections [10], there are experimental difficulties in preparing the targets. Therefore, it is challenging to synthesize superheavy elements greater than $Z = 118$ using ^{40,48}Ca as a projectile. Recent detailed studies on alpha decay and fusion between different projectile and target combinations have shown the production of superheavy elements $Z = 121$ in the mass number range of 265–316 [11]. Studying a combined dynamic and statistical model, previous researchers [12] predicted the production cross section for superheavy elements in the atomic number range $104 \leq Z \leq 112$. Earlier

✉ H. C. Manjunatha
manjunathhc@rediffmail.com

✉ N. Sowmya
sowmyaprakash8@gmail.com

1 Department of Physics, R V College of Engineering, Bangalore 560074, India

2 Visvesvaraya Technological University, Belagavi, Karnataka 590018, India

3 Department of Physics, Government First Grade College, Srinivasapur, Karnataka 563135, India

4 Department of Physics, Government First Grade College, Devanahally, Karnataka 562110, India

5 Department of Physics, Government First Grade College, Mulbagal, Karnataka 563131, India

6 Department of Physics, Government First Grade college, Nanjangud, Ooty Road, Mysore 571301, India

researchers predicted the production cross sections of superheavy elements $Z \geq 104$ using a statistical model [13–17].

By considering the angular orientations of the projectile and target nuclei in the reactions, the production cross sections can be maximized [18]. ^{48}Ca-induced hot fusion reactions, such as ^{48}Ca+^{236}Np, ^{242}Am, and ^{248}Bk, produce odd superheavy elements with atomic numbers 113, 115, and 117 [19]. ^{48}Ca has been extensively used in the synthesis of isotopes with $Z = 115$, and its decay properties have been measured [7]. Furthermore, studies have been conducted on actinide targets, such as ^{238}U, ^{242}Pu, ^{244}Pu, ^{243}Am, ^{245}Cm, ^{249}Cf, ^{249}Bk, and ^{48}Ca beams, as projectiles to synthesize superheavy elements from $Z = 113$ to 118 using the hot fusion technique [20]. The microscopic approach based on the time-dependent Hartree–Fock theory (TDHF) [21] and the Langevin approach have been developed to synthesize the superheavy element $Z = 120$ with hot fusion reaction systems such as ^{48}Ca+^{257}Fm, ^{51}V+^{249}Bk, ^{54}Cr+^{248}Cm[22]. Earlier researchers anticipated the production cross sections, optimal energy, quasifission, and fusion-fission lifetimes of superheavy elements in the region $104 \leq Z \leq 120$ using a dinuclear system model [23–26].

Recent investigations have shown that instead of using ^{48}Ca as a projectile, Ti, Cr, and Fe beams can be used as projectiles with actinide targets to produce superheavy elements through processes such as accelerated fission fragments process and multi-nucleon transfer process [27]. Hence, based on detailed investigations, we were motivated to explore $^{50,52-54}$Cr-induced fusion reactions on targets from Hg to Cf for the formation of superheavy elements in the atomic number range $104 \leq Z \leq 122$ using a statistical model.

The theory used to predict evaporation residue cross sections using the statistical model is given in Sect. 2. The results obtained using $^{50,52-54}$Cr-induced fusion reactions are presented in Sect. 3. The conclusions drawn from this study are presented in Sect. 4.

2 Theoretical Framework

The total potential for $^{50,52-54}$Cr-induced fusion reactions is evaluated as follows:

$$V(R) = V_C(R) + V_N(R) + \frac{\ell(\ell+1)}{2\mu \times R^2}. \tag{1}$$

The Coulomb interaction potential ($V_C(R)$) and nuclear interaction potential ($V_N(R)$) [23] are expressed as

$$V_C(R) = \frac{e^2 Z_1 Z_2}{R} \tag{2}$$

and

$$V_N(R) = \frac{V_0}{1 + \exp[(R - R_0)/a]}. \tag{3}$$

In Eqs. 2 and 3, Z_1 and Z_2 are the atomic numbers of the projectile and the target, respectively. $e^2 \approx 1.44$, a is the diffuseness parameter, and R_0 is the minimum nuclear potential distance. R_0 and V_0 are evaluated as described in literature [28]. The above potential focuses on fusion-fission reactions, minimizing the role of quasi-fission. It employs a modified Woods–Saxon potential based on the Skyrme energy density functional and an extended Thomas–Fermi approach. The modified Woods (MWS) potential model, built on previous successful descriptions of fusion reactions, transitioned from a numerically computed entrance channel potential to a practical analytical expression. This analytical MWS potential streamlines the investigation of the fusion and fission barriers, thereby improving their practical utility. $\frac{\ell(\ell+1)}{2\mu \times R^2}$ denotes the centrifugal potential. The average angular momentum $\langle J \rangle$ is deduced from [29]:

$$\langle \ell \rangle = \begin{cases} \frac{2}{3}\sqrt{2\mu R_B^2 (E_{cm} - V_B)/\hbar^2} & \text{for } E_{cm} \geq V_B \\ \frac{4}{3}\sqrt{2\mu R_B^2\, \epsilon/\hbar^2} & \text{for } E_{cm} < V_B \end{cases} \tag{4}$$

where μ is the reduced mass of the projectile and target nuclei, and R_B is the barrier radius. E_{cm} are the center of mass energy and the fusion barrier height, respectively.

The boundary conditions used to determine the determination of fusion barrier position (R_B) and height (V_B) are explained in [30]. The evaporation cross section of the superheavy nuclei with consequent light particle emission is represented as follows:

$$\sigma_{ER}^{xn} = \frac{\pi}{k^2} \sum_{\ell=0}^{\infty} (2\ell+1) T(E,\ell) P_{CN}(E^*,\ell) P_{sur}^{xn}(E^*,\ell), \tag{5}$$

where k, ℓ and $T_\ell(E_{cm})$ have the same notation. In the above equation, P_{CN} is evaluated as follows:

$$P_{CN}(E^*,\ell) = \frac{\exp[-c(\chi_{eff} - \chi_{thr})]}{1 + \exp\left(\frac{E_B^* - E^*}{\Delta}\right)}. \tag{6}$$

where the compound nucleus excitation energy is denoted by E^* and E_B^*, when E_{cm} (the center of mass energy) is equal to the Coulomb and proximity barriers. Δ, χ_{thr} and c are adjustable parameters, χ_{eff} is the effective fissility [17] is as follows:

$$\chi_{eff} = \left[\frac{(Z^2/A)}{(Z^2/A)_{crit}}\right][1 - \alpha + \alpha f(\phi)], \tag{7}$$

where $(Z^2/A)_{crit}$, $f(\phi)$, and ϕ are expressed as:

$$(Z^2/A)_{\text{crit}} = 50.883\left[1 - 1.7286\left(\frac{(N-Z)^2}{A}\right)\right], \tag{8}$$

$$f(\phi) = \frac{4}{\phi^2 + \phi + \frac{1}{\phi} + \frac{1}{\phi^2}}, \tag{9}$$

and

$$\phi = (A_1 + A_2)^{1/3}, \tag{10}$$

A, N, and Z are the mass, neutron number, and atomic number of the compound nuclei, respectively. A_1 and A_2 are the masses of the projectile and target nuclei, respectively. $T_\ell(E_{\text{cm}})$ is evaluated as

$$T_\ell(E_{\text{cm}}) = \left[1 + \exp\left(\frac{2\pi}{\hbar\omega_\ell}(V_{\text{B}} - E_{\text{cm}})\right)\right]^{-1}, \tag{11}$$

where $\hbar\omega_\ell$ is the inverted parabola and V_{B} is the fusion barrier height. Both $\hbar\omega_\ell$ and V_{B} are evaluated using a set of equations explained in the literature [31]. E_{cm} is the center of mass energy and the compound nucleus probability P_{CN} is evaluated as explained in the literature [32]. The survival probability $P^{xn}_{\text{sur}}(E^*, \ell)$ is expressed as

$$P^{xn}_{\text{sur}}(E^*_{\text{CN}}, \ell) = P_{xn}(E^*) \prod_{i=1}^{i_{\max}=x} \left(\frac{\Gamma_n(E^*_{\text{CN}}, \ell)}{\Gamma_n(E^*_{\text{CN}}, \ell) + \Gamma_f(E^*_{\text{CN}}, \ell)}\right)_{i,E^*}, \tag{12}$$

where $\Gamma_n(E^*_{\text{CN}}, \ell)$ is the decay width of neutrons, and $\Gamma_f(E^*_{\text{CN}}, \ell)$ is the fission decay width. The decay width was calculated as follows:

$$\Gamma_i = \frac{R_{CN_i}}{2\pi\rho(E^*_{\text{CN}})}, \tag{13}$$

the level density at saddle point is denoted by $\rho_{\text{f}}(E^*_{\text{CN}} - B_{\text{f}} - \epsilon, \ell)$, $\hbar\omega = 2.2$ MeV [33], and B_{f} is the fission barrier [34]. The level density [35] is expressed as follows:

$$\begin{aligned}\rho(E^*, \ell) =& K_{\text{vib}}(E^*)K_{\text{rot}}(E^*)\\ &\times \frac{2\ell + 1}{24\sqrt{2}\sigma^3_{\text{eff}}[a(A, E^* - E_{\text{c}})(E^* - E_{\text{c}})^5]^{1/4}}\\ &\times \exp\left[2\sqrt{a(A, E^* - E_{\text{c}})(E^* - E_{\text{c}})} - \frac{(\ell + 1/2)^2}{2\sigma^2_{\text{eff}}}\right],\end{aligned} \tag{14}$$

where E_{c}, σ_{eff}, K_{rot} and K_{vib} are the usual notations explained in detail in [35]. The perpendicular ($\mathfrak{I}_\perp$) and parallel ($\mathfrak{I}_\parallel$) moments of inertia are evaluated as previously described [23].

The level density ($a(A, E^* - E_{\text{c}})$) is expressed as

Table 1 Tabulation of evaporation residue cross sections using ^{54}Cr-projectiles on lead and bismuth targets, evaporation residue channel, the center of mass energy, and production cross sections of experiments [36, 37] and current study

Reaction	E_{cm} (MeV)	EVR (pb)	
		Expt	PW
^{54}Cr(^{208}Pb, 1n)^{261}Sg	200	2233	1975
^{54}Cr(^{208}Pb, 1n)^{261}Sg	202	2520	2105
^{54}Cr(^{208}Pb, 1n)^{261}Sg	204	1169	980
^{54}Cr(^{208}Pb, 1n)^{261}Sg	205	716	621
^{54}Cr(^{208}Pb, 1n)^{261}Sg	209	180	158
^{54}Cr(^{208}Pb, 1n)^{261}Sg	212	84	64
^{54}Cr(^{208}Pb, 2n)^{260}Sg	205	116	115
^{54}Cr(^{208}Pb, 2n)^{260}Sg	209	504	513
^{54}Cr(^{208}Pb, 2n)^{260}Sg	212	479	140
^{54}Cr(^{208}Pb, 3n)^{259}Sg	219	10	11
^{54}Cr(^{209}Bi, 1n)^{262}Bh	206	163	122
^{54}Cr(^{209}Bi, 1n)^{262}Bh	210	27	13
^{54}Cr(^{209}Bi, 2n)^{261}Bh	206	36	25
^{54}Cr(^{209}Bi, 2n)^{261}Bh	210	36	24
^{54}Cr(^{209}Bi, 2n)^{261}Bh	214	24	26

$$a(A, E^* - E_{\text{c}}) = \tilde{a}(A)\left[1 + \frac{1 - \exp[-(E^* - E_{\text{c}})/E'_{\text{D}}]}{E^* - E_{\text{c}}}\delta W\right]. \tag{15}$$

Here, we take the values $E'_{\text{D}} = 18.5$ MeV and $\tilde{a}(A) = 0.114A + 0.162A^{2/3}$.

3 Results and discussion

Using a $^{50,52-54}$Cr projectile, a search was conducted to find acceptable targets with a longer half-life for the synthesis of the superheavy elements in the region $104 \le Z \le 122$. In this regard, we observed more stable Hg–Cf isotopes with longer half-lives. Consequently, in subsequent studies, we explored the fusion reactions using Hg-to-Cf isotopes as the target and $^{50,52-54}$Cr as the projectile. The fusion cross section [28] is evaluated as follows.

$$\sigma^{\text{Wang}}_{\text{fus}}(E_{\text{cm}}, B) = \frac{\hbar\omega R^2_{\text{B}}}{2E_{\text{cm}}} \ln\left(1 + \exp\left[\frac{2\pi}{\hbar\omega}(E_{\text{cm}} - V_{\text{B}})\right]\right) \tag{16}$$

where E_{cm}, V_{B}, R_{B} and $\hbar\omega$ are the center of mass energy, barrier height, barrier radius, and barrier curvature, respectively. Furthermore, the evaporation residue cross sections were evaluated, as explained in Sect. 2.

The evaporation residue cross sections are validated by comparing them with those from available experiments.

Table 1 shows a comparison of ^{54}Cr projectiles on ^{208}Pb and ^{209}Bi targets with the available experimental values [36, 37]. The prediction of the theoretical model was successful when the findings agreed with the experimental values. Table 1 shows the σ_{EVR} for ^{208}Pb and ^{209}Bi targets using ^{54}Cr projectile. Notably, the agreement between the predicted and experimental values is good for ^{54}Cr+^{208}Pb and ^{54}Cr+^{209}Bi. Hence, the current model is more reliable for the prediction of cross sections in the superheavy element region $104 \leq Z \leq 122$ using Cr projectiles. Therefore, with the confidence of reproducing the experimental evaporation residue cross sections, we extended our studies to $^{50,52-54}$ Cr projectiles on different targets. Therefore, we considered the stable isotopes of targets ranging from mercury to californium. In each fusion reaction case, the evaporation residue cross section was evaluated, and its optimal energy was identified, as explained in the literature [26]. Optimal energy is the energy corresponding to the maximum evaporation residue cross section. Hence, in each Cr-induced fusion reaction, the optimal energy at which the maximum evaporation residue cross section was considered.

Furthermore, we plotted fusion cross section as a function of the atomic number of compound nuclei and it is illustrated in Fig. 1. The fusion cross sections for ^{50}Cr projectile on different targets at optimal energies are illustrated in Fig. 1a. The figure shows that a larger fusion cross section is observed for $Z_c = 106$ and the minimum fusion cross section is observed for $Z_c = 112$. From Fig. 1a, it is clear that the fusion cross sections increase and are maximum for $Z_c = 106$ and then gradually decrease and reach a minimum when $Z_c = 112$. In addition, σ_{fus} gradually increases. Similar results were observed for ^{52,53,54}Cr-induced fusion reactions, as shown in Fig. 1b–d. In all these cases, σ_{fus} is maximized when $Z_c = 104$ and $Z_c = 106$ for ^{52,53}Cr and ^{54}Cr, respectively. The maximum values of σ_{fus} are owing to the presence of numerous atomic/neutron compound nuclei.

First, the value of P_{CN} is determined by the competition between complete fusion and quasifission. The formed compound nuclei were excited because the beam energy of the projectile (E_{cm}) was often higher than the Q value for the production of the compound nuclei. Hence, we investigated the effect of magic numbers on P_{CN} for superheavy elements in the region $104 \leq Z_c \leq 122$, as shown in Fig. 2a–d. Despite the effect of the atomic number on the fusion cross sections, we also investigated P_{CN} as a function of the target nuclei. From Fig. 2a, it can be observed that P_{CN} is the maximum when A_T =248 for which $Z_T = 96$ and $N_T = 152$. Similarly, for ^{52} and ^{54}Cr-induced fusion reactions, we observed a larger P_{CN} when $A_T = 248$. However, we observe a larger P_{CN} for $A_T = 249$, with $N_T = 151$ and $Z_T = 98$.

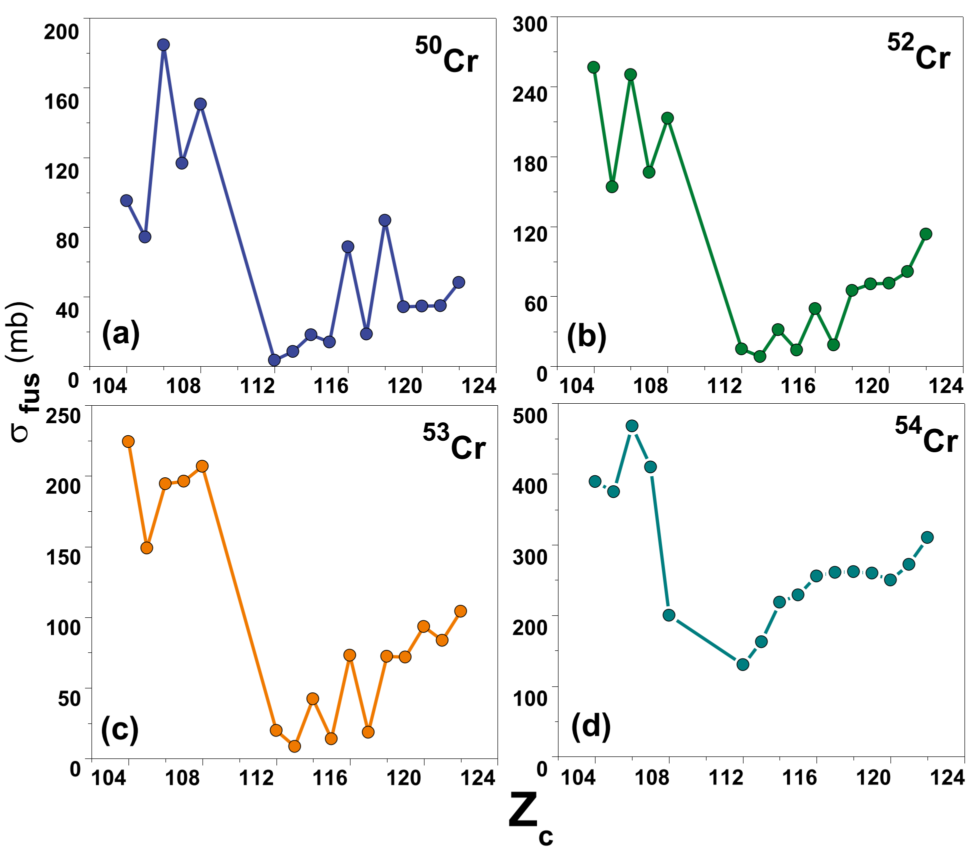

Fig. 1 A plot of fusion cross sections for $^{50,52-54}$Cr-induced fusion reactions at optimal energies as a function of the atomic number of compound nuclei leading to the formation of superheavy elements in the region $104 \leq Z \leq 122$

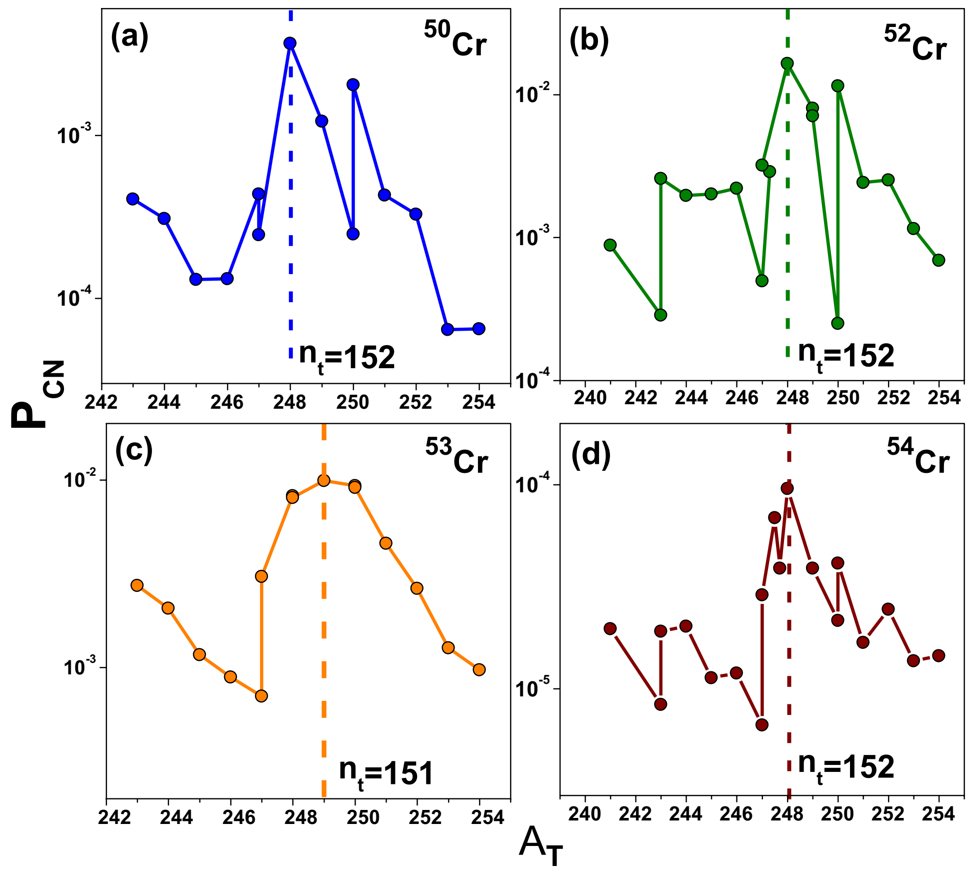

Fig. 2 A plot of compound nucleus formation probability for $^{50,52-54}$Cr-induced fusion reactions at optimal energies as a function of the mass number of compound nuclei leading to the formation of superheavy elements in the region $104 \leq Z \leq 122$

In the literature [30, 38], remarkable contribution has been observed related to the Coulomb interaction parameter. Hence, we investigated the effect of the Coulomb interaction parameter $\left(z = \frac{Z_1 Z_2}{A_1^{1/3}+A_2^{1/3}}\right)$ on the Cr-induced fusion reactions, leading to the formation of compound nuclei in the region $104 \leq Z \leq 122$ as shown in Fig. 3a–d. For each fusion reaction, we considered P_{CN}-value at the optimal beam energy. The P_{CN} value increases with the Coulomb interaction parameters. The value of P_{CN} was found to be smaller when z was approximately 344 and larger when $Z = 353$ in the case of $^{50,52-54}$Cr-induced fusion reactions. Hence, P_{CN} gradually increases with an increase in the Coulomb interaction parameter.

In the second step of the process, the compound nucleus loses excitation energy predominantly by light particles and γ-emission. One of the most important considerations in the production of heavy and superheavy elements is the probability of the compound nucleus surviving fission during the de-excitation process. Hence, we further investigated the survival probability for each fusion reaction and considered P_{sur} at the optimal energies. P_{sur} is evaluated as explained in Eq. 12, where the neutron decay width and fission decay width are estimated as explained in the Theory section. Figure 4a–d shows a plot of survival probability as a function of the atomic number of superheavy elements in the region $104 \leq Z \leq 122$ using $^{50,52-54}$Cr-induced fusion reactions. Here, the value of P_{sur} increases with Z_C. Furthermore, additional stability was observed when the formed compound nuclei acquired an even atomic number, as shown in the figure. A compound system with an even number of protons or neutrons exhibits comparatively high stability [39]. An even nucleus will have a more symmetric distribution of protons and neutrons, leading to enhanced binding energy and contributing to greater stability and a higher survival probability than the neighboring odd-numbered nuclei. In agreement with these results, it was also observed that the survival probability for even atomic numbers of compound nuclei is comparatively larger than that of their neighboring odd-number nucleons in the compound nucleus.

Finally, superheavy nuclei will be formed with the liberation of light particles such as neutrons/gamma/alpha particles. Figure 5a–d shows a plot of evaporation residue cross sections for 2n, 3n, and 4n evaporation channels as a function of the center of mass energy for ^{53}Cr+^{243}Am, ^{54}Cr+^{247}Cm, ^{53}Cr+^{248}Bk, and ^{53}Cr+^{250}Cf, respectively. In all cases, we recognized a larger cross section for the 3n evaporation channel, and the energy at which the maximum cross section was observed was the optimal energy.

Fig. 3 A plot of compound nucleus formation probability for $^{50,52-54}$Cr-induced fusion reactions at optimal energies as a function of Coulomb interaction parameter leading to the formation of compound nuclei in the region $104 \le Z \le 122$

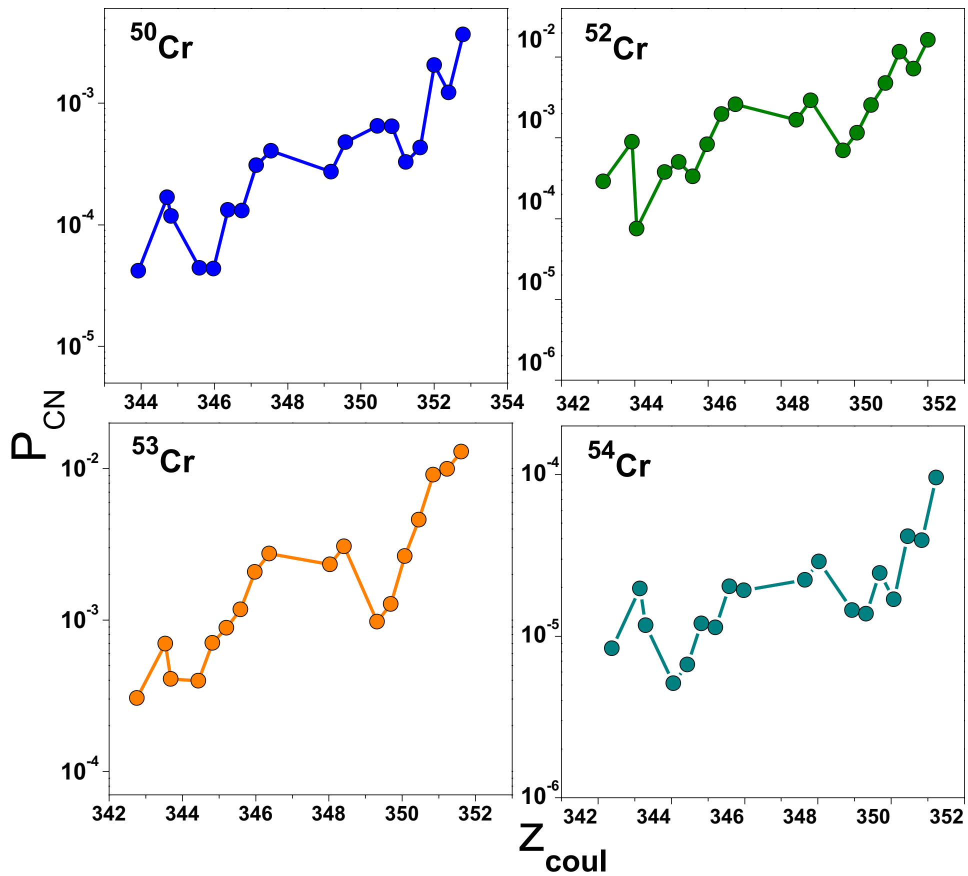

Fig. 4 A plot of survival probability for $^{50,52-54}$Cr-induced fusion reactions at optimal energies as a function of the atomic number of superheavy elements in the region $104 \le Z \le 122$

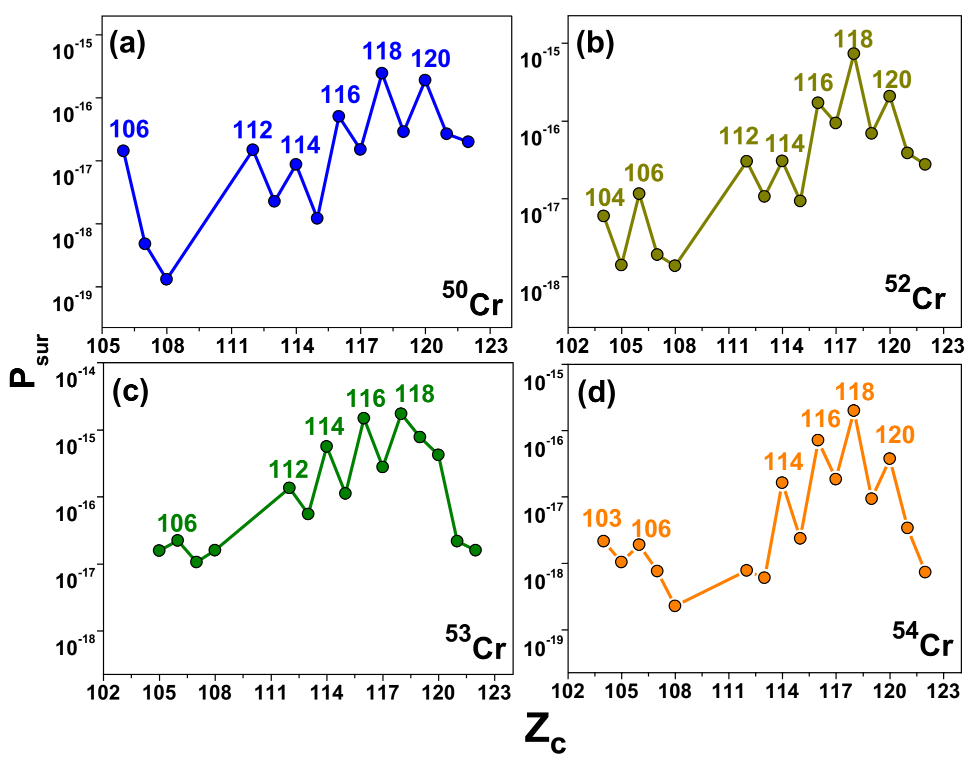

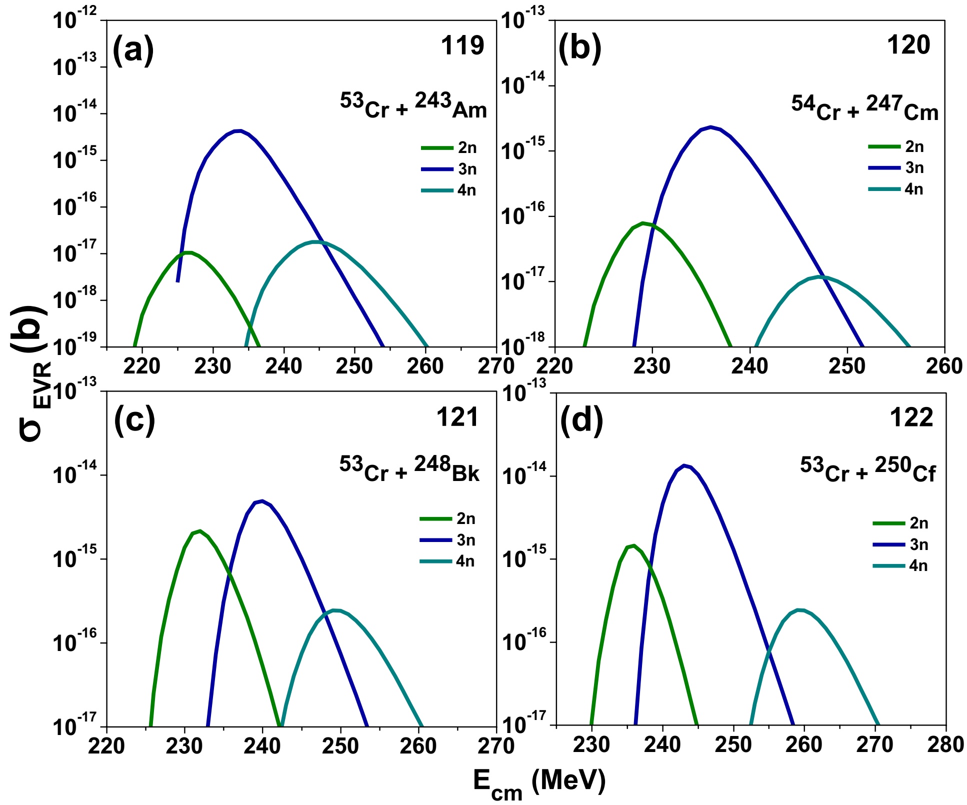

Fig. 5 A plot of evaporation residue cross sections as a function of center of mass energy for the fusion reactions of **a** $^{53}Cr+^{243}Am$, **b** $^{54}Cr+^{247}Cm$, **c** $^{53}Cr+^{248}Bk$, and **d** $^{53}Cr+^{250}Cf$ leading to the formation of superheavy elements $Z = 119$, 120, 121 and 122 respectively

The predicted cross sections were 42fb at 236 MeV for $^{53}Cr+^{243}Am$, 23.2 fb at 236 MeV for $^{54}Cr+^{247}Cm$, 95.6 fb at 240 MeV for $^{53}Cr+^{248}Bk$, and 1.33 fb at 242 MeV for $^{53}Cr+^{250}Cf$. The larger cross sections for ^{53}Cr and ^{54}Cr-induced fusion reactions are owing to their stability, which is advantageous for experimental purposes. They did not undergo radioactive decay during the experiment, thus providing a more stable environment for the experimentalist. Additionally, these isotopes are readily available, making them practical choices for experimental setups. Furthermore, we tabulated the predicted cross sections for the unexplored isotopes of superheavy elements $Z = 119$ and 120, as provided in Table 2. Additionally, the optimal energy obtained in the current study was compared with the prediction from Eq. (8) in Ref. [40].

Furthermore, we plotted evaporation residue cross sections as a function of the atomic number of compound nuclei during the 3n evaporation channel and it is shown in Fig. 6. The evaporation residue cross sections decreased with an increase in the atomic number of the compound nuclei. However, a larger cross section was observed for $Z = 121$. Hence, these predicted cross sections with excitation and beam energies are important for future experiments on Cr-induced fusion reactions.

Table 2 Tabulation of fusion reactions, fusion barrier height, excitation energy, and evaporation residue cross sections for superheavy elements $Z = 119$ and 120

Fusion reaction	V_B (MeV)	E_{cm}^{opt}(MeV)		E^* (MeV)	σ_{evr} (fb)
		PW	[40]		
$^{50}Cr(^{243}Am,3n)^{290}Uue$	232.1	230.3	230	29.7	0.422
$^{52}Cr(^{243}Am,3n)^{292}Uue$	230.9	236.7	235	35.1	3.44
$^{53}Cr(^{243}Am,3n)^{293}Uue$	230.8	236.2	236	33.3	42
$^{54}Cr(^{243}Am,3n)^{294}Uue$	229.8	238.9	236	42.8	7.79
$^{50}Cr(^{247}Cm,3n)^{294}Ubn$	233.8	229.9	229	25.6	1.28
$^{52}Cr(^{245}Cm,3n)^{294}Ubn$	232.9	239.9	237	36.7	7.6
$^{53}Cr(^{248}Cm,3n)^{298}Ubn$	231.8	236.8	234	30.5	16.7
$^{54}Cr(^{247}Cm,3n)^{298}Ubn$	213.4	239.9	236	36.5	23.2
$^{50}Cr(^{248}Bk,3n)^{295}Ubu$	236.3	236.5	235	28.6	0.49
$^{52}Cr(^{248}Bk,3n)^{297}Ubu$	234.9	243.2	239	31.7	1.91
$^{53}Cr(^{248}Bk,3n)^{298}Ubu$	234.4	244.1	240	31	95.6
$^{54}Cr(^{248}Bk,3n)^{299}Ubu$	233.8	245.7	241	35.5	3.13
$^{50}Cr(^{249}Cf,3n)^{296}Ubb$	239.1	242.7	240	31.5	0.211
$^{52}Cr(^{251}Cf,3n)^{300}Ubb$	237.1	245.5	241	29.6	1.31
$^{53}Cr(^{250}Cf,3n)^{300}Ubb$	236.7	248.4	242	27.9	1.33
$^{54}Cr(^{249}Cf,3n)^{300}Ubb$	236.3	250.9	247	28.4	0.99

Additionally, the optimal energy obtained from the current study is compared with the prediction from Eq. (8) in reference [40]

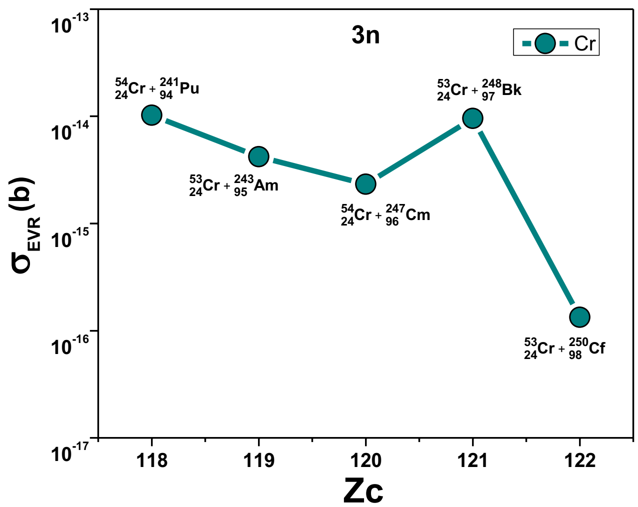

Fig. 6 A plot of evaporation residue cross sections for the 3n channel as a function of atomic number of compound nuclei

4 Conclusion

We studied $^{50,52-54}$Cr-induced fusion reactions for the synthesis of superheavy element in the $104 \le Z \le 122$ range. The barrier height and position were determined using boundary conditions, in which the total potential was equal to the sum of the Coulomb, nuclear, and centrifugal potentials. The cross sections obtained in this study using ^{54}Cr projectiles were compared to those obtained in previous studies. The projected cross sections from this study are in good agreement with the results of previous investigations. Detailed investigations revealed that the survival probability is more stable when the atomic number of the compound nuclei is even. Consequently, these projected cross sections with excitation and beam energies will be useful in future Cr-induced fusion reaction investigations.

Declarations

Conflict of interest The authors declare that they have no conflict of interest.

References

1. D.N. Schramm, W.A. Fowler, Synthesis of superheavy elements in the r-process. Nature **231**, 103–106 (1971). https://doi.org/10.1038/231103a0
2. G.T. Seaborg, W. Lovel, D. Morrissey et al., Superheavy elements: a crossroads. Science **4382**, 711–717 (1979). https://doi.org/10.1126/science.203.4382.711
3. S. Hofmann, Synthesis of superheavy elements by cold fusion. Radiochim. Acta **99**, 405–428 (2011). https://doi.org/10.1524/ract.2011.1854
4. S. Hofmann, V. Ninov, F.P. Berger et al., The new element 112. Z. Phys. A Hadron. Nucl. **354**, 229–230 (1996). https://doi.org/10.1007/BF02769517
5. J. Khuyagbaatar, A. Yakushev, C.E. Düllmann et al., Fusion reaction ^{48}Ca+^{249}Bk leading to formation of the element Ts (Z=117). Phys. Rev. C **99**, 054306 (2019). https://doi.org/10.1103/PhysRevC.99.054306
6. YuTs. Oganessian, V.K. Utyonkov, Yu.V. Lobanov et al., Synthesis of superheavy nuclei in the ^{48}Ca+ ^{244}Pu reaction. Phys. Rev. Lett. **83**, 3154 (1999). https://doi.org/10.1103/PhysRevLett.83.3154
7. YuTs. Oganessian, V.K. Utyonkov, Yu.V. Lobanov et al., Experiments on the synthesis of element 115 in the reaction ^{243}Am(^{48}Ca, xn) $^{291-x}$115. Phys. Rev. C **69**, 021601 (2004). https://doi.org/10.1103/PhysRevC.69.021601
8. S. Chopra, N. Goel, M. Sharma et al., Theoretical attempt to predict the cross sections in the case of new superheavy elements. Phys. Rev. C **106**, L031601 (2022). https://doi.org/10.1103/PhysRevC.106.L031601
9. G.G. Adamian, N.V. Antonenko, W. Scheid et al., Characteristics of quasifission products within the dinuclear system model. Phys. Rev. C **68**, 034601 (2003). https://doi.org/10.1103/PhysRevC.68.034601
10. F. Li, L. Zhu, Z.-H. Wu et al., Predictions for the synthesis of superheavy elements $Z = 119$ and 120. Phys. Rev. C **98**, 014618 (2018). https://doi.org/10.1103/PhysRevC.98.014618
11. K.N. Sridhar, H.C. Manjunatha, H.B. Ramalingam et al., Search for possible fusion reactions to synthesize the superheavy element $Z = 121$. Phys. Rev. C **98**, 064605 (2018). https://doi.org/10.1103/PhysRevC.98.064605
12. G. Giardina, S. Hofmann, A.I. Muminov et al., Effect of the entrance channel on the synthesis of superheavy elements. Eur. Phys. J. A **8**, 205–216 (2000). https://doi.org/10.1007/s10050-000-4509-7
13. H.C. Manjunatha, K.N. Sridhar, N. Sowmya et al., Investigations of the synthesis of the superheavy element $Z = 122$. Phys. Rev. C **98**, 024308 (2018). https://doi.org/10.1103/PhysRevC.98.024308
14. H.C. Manjunatha, N. Sowmya, N. Manjunatha et al., Entrance channel dependent hot fusion reactions for superheavy element synthesis. Phys. Rev. C **102**, 064605 (2020). https://doi.org/10.1103/PhysRevC.102.064605
15. H.C. Manjunatha, K.N. Sridhar, N. Sowmya et al., Investigations on $^{64}Ni{+}_{Z}An^{A} \rightarrow_{Z=104-123} (SHN)^{A=250-310}$ reactions. Nucl. Phys. A **987**, 382–395 (2019). https://doi.org/10.1016/j.nuclphysa.2019.05.006
16. H.C. Manjunatha, N. Sowmya, P.S. Damodara, Synthesis of superheavy elements using krypton and argon beams. Indian J. Phys. **97**, 869–877 (2023). https://doi.org/10.1007/s12648-022-02430-z
17. H.C. Manjunatha, L. Seenappa, N. Sowmya et al., Investigations on $^{54-60}$ Fe $+^{238-244}$ Pu $\rightarrow^{296-302}$120 fusion reactions. Can. J. Phys. **99**, 16–23 (2021). https://doi.org/10.1139/cjp-2019-0580
18. G. Giardina, A.I. Muminov, G. Mandaglio et al., Peculiarities of nuclear fusion in synthesis of superheavy elements. J. Nucl. Radiochem. Sci. **8**, 63–67 (2007). https://doi.org/10.1139/cjp-2019-0580
19. G. Adamian, N.V. Antonenko, W. Scheid et al., Possibilities of synthesis of new superheavy nuclei in actinide-based fusion reactions. Phys. Rev. C **69**, 044601 (2004). https://doi.org/10.1103/PhysRevC.69.044601
20. J.B. Roberto, C.W. Alexander, R.A. Boll et al., Actinide targets for the synthesis of super-heavy elements. Nucl. Phys. A **944**, 99–116 (2015). https://doi.org/10.1016/j.nuclphysa.2015.06.009
21. K. Godbey, A.S. Umar, Quasifission dynamics in microscopic theories. Front. Phys. **8**, 40 (2020). https://doi.org/10.3389/fphy.2020.00040

22. K. Sekizawa, K. Hagino, Time-dependent Hartree–Fock plus Langevin approach for hot fusion reactions to synthesize the $Z = 120$ superheavy element. Phys. Rev. C **99**, 051602 (2019). https://doi.org/10.1103/PhysRevC.99.051602
23. H.C. Manjunatha, P.S. Damodara Gupta, N. Sowmya et al., Systematics of heavy ion fusion with entrance channel and deformation parameters. Phys. Rev. C **104**, 024622 (2021). https://doi.org/10.1103/PhysRevC.104.024622
24. P.S. Damodara Gupta, N. Sowmya, H.C. Manjunatha et al., Quasi-fission barrier of heavy ion fusion reactions leading to the formation of the superheavy nucleus ^{302}120. Phys. Rev. C **106**, 064603 (2022). https://doi.org/10.1103/PhysRevC.106.064603
25. H.C. Manjunatha, L. Seenappa, P.S. DamodaraGupta et al., Quasi-fission and fusion-fission lifetime studies for the superheavy element $Z = 120$. Phys. Rev. C **103**, 024311 (2021). https://doi.org/10.1103/PhysRevC.103.024311
26. H.C. Manjunatha, N. Sowmya, P.S. Damodara Gupta et al., Role of optimal beam energies in the heavy ion fusion reaction. Eur. Phys. J. Plus **137**, 693 (2022). https://doi.org/10.1140/epjp/s13360-022-02677-9
27. V. Zagrebaev, W. Greiner, Role of optimal beam energies in the heavy ion fusion reaction. Phys. Rev. C **78**, 034610 (2008). https://doi.org/10.1103/PhysRevC.78.034610
28. N. Wang, K. Zhao, W. Scheid et al., Fusion-fission reactions with a modified Woods–Saxon potential. Phys. Rev. C **77**, 014603 (2008). https://doi.org/10.1103/PhysRevC.77.014603
29. O.A. Capurro, D.E. DiGregorio, S. Gil et al., Average angular momentum in compound nucleus reactions deduced from isomer ratio measurements. Phys. Rev. C **55**, 766–774 (1997). https://doi.org/10.1103/PhysRevC.55.766
30. P.S. Damodara Gupta, N. Sowmya, H.C. Manjunatha et al., Investigations on the synthesis of different isotopes of uranium using fusion reactions. Braz. J. Phys. **51**, 1803–1809 (2021). https://doi.org/10.1007/s13538-021-00973-w
31. H.C. Manjunatha, K.N. Sridhar, N. Nagaraja et al., Pocket formula for fusion barriers of superheavy nuclei. Eur. Phys. J. Plus **133**, 227 (2018). https://doi.org/10.1140/epjp/i2018-12057-3
32. H.C. Manjunatha, P.S. Damodara Gupta, N. Sowmya et al., Empirical model for compound nucleus formation probability in heavy ion fusion reactions. Eur. Phys. J. Plus **138**, 528 (2023). https://doi.org/10.1140/epjp/s13360-023-04022-0
33. N. Sowmya, P.S. Damodara Gupta, H.C. Manjunatha et al., Accurately estimated neutron and fission decay widths for hot fusion reactions. Phys. Rev. C **105**, 044605 (2022). https://doi.org/10.1103/PhysRevC.105.044605
34. P. Moller, A.J. Sierk, T. Ichikawa et al., Heavy-element fission barriers. Phys. Rev. C **79**, 064304 (2009). https://doi.org/10.1103/PhysRevC.79.064304
35. A.S. Zubov, G.G. Adamian, N.V. Antonenko et al., Survival probability of superheavy nuclei. Phys. Rev. C **65**, 024308 (2002). https://doi.org/10.1103/PhysRevC.65.024308
36. S. Hofmann, Properties of heavy nuclei measured at the GSI SHIP. AIP Conf. Proc. **704**, 21–30 (2004). https://doi.org/10.1063/1.1737093
37. G. Münzenberg, S. Hofmann, F.P. Heßberger et al., Identification of element 107 by α correlation chains. Z. Phys. A Atoms Nucl. **300**, 107–108 (1981). https://doi.org/10.1007/BF01412623
38. A. Kaur, S. Chopra, R.K. Gupta et al., Compound nucleus formation probability P_{CN} determined within the dynamical cluster-decay model for various "hot'' fusion reactions. Phys. Rev. C **90**, 024619 (2014). https://doi.org/10.1103/PhysRevC.90.024619
39. N.K. Virk, M.K. Sharma, R. Kumar et al., Role of shell and pairing correction in the dynamics of compound nuclei with A_{CN} =118-196 using collective clusterization approach. Nucl. Phys. A **981**, 89–106 (2019). https://doi.org/10.1016/j.nuclphysa.2018.10.059
40. L. Zhu, Law of optimal incident energy for synthesizing superheavy elements in hot fusion reactions. Phys. Rev. Res. **5**, L022030 (2023). https://doi.org/10.1103/PhysRevResearch.5.L022030